THE ASTROPHYSICAL JOURNAL, 464:131–140, 1996 June 10

SUPERSONIC COLLISIONS BETWEEN TWO GAS STREAMS

HYUNG MOK LEE AND HYESUNG KANG
Department of Earth Sciences, Pusan National University, Pusan 609-735, Korea;
hmlee@astrophys.es.pusan.ac.kr, kang@astrophys.es.pusan.ac.kr

AND

DONGSU RYU
Department of Astronomy and Space Science, Chungnam National University, Daejeon 305-764, Korea;
ryu@sirius.chungnam.ac.kr
Received 1995 October 16; accepted 1995 December 28

ABSTRACT

A star around a massive black hole can be disrupted tidally by the gravity of the black hole. Then its debris may form a precessing stream, which may even collide with itself. In order to understand the dynamical effects of the stream-stream collision on the eventual accretion of the stellar debris onto the black hole, we have studied how the gas flow behaves when the outgoing stream collides supersonically with the incoming stream. We have investigated the problem analytically with one-dimensional plane-parallel streams and numerically with more realistic, three-dimensional streams. A shock formed around the contact surface converts the bulk of the orbital streaming kinetic energy into thermal energy. In three-dimensional simulations, the accumulated, hot postshock gas then expands adiabatically and drives another shock into the low-density ambient region. Through this expansion, thermal energy is converted back to the kinetic energy associated with the expanding motion. Thus, in the end, only a small fraction of the orbital kinetic energy is actually converted to thermal energy, while most of it is transferred to the kinetic energy of the expanding gas. Nevertheless, the collision is effective in circularizing the debris' orbit because the shock efficiently transforms the ordered motion of the streams into the expanding motion in directions perpendicular to the streams. The circularization efficiency decreases if two colliding streams have a large ratio of cross sections and a large density contrast. But even in such cases, the main shock extends beyond the overlapping contact surface, and the high-pressure region behind the shock keeps the stream of the larger cross section from passing freely. Thus stream-stream collisions are still expected to circularize the stellar debris rather efficiently, unless the ratio of the cross sections is very large (i.e., $\sigma_1/\sigma_2 \gg 10$).

Subject headings: black hole physics — galaxies: nuclei — hydrodynamics — shock waves

1. INTRODUCTION

It is believed that the tidal disruption of stars can occur at a rate of approximately one every 10^4 yr in typical nuclei of nearby galaxies with observational evidence for a supermassive black hole (see, e.g., Rees 1988; Cannizzo, Lee, & Goodman 1990). A large amount of energy ($\sim 0.1 m_* c^2$) can be released if a significant fraction of the stellar mass is accreted onto the black hole. However, galaxies with convincing dynamical evidence for a central black hole usually do not reveal strong activity in their central parts (i.e., large M/L). It is possible that the dynamical mass implied by spectroscopic observations might be due not to a massive black hole but to a cluster of dark stars (Goodman & Lee 1989). High-resolution observations in the near future would enable us to eliminate some candidates for the constituents of dark clusters. It is, however, too early to rule out the existence of a central, massive black hole on the grounds of low-level activity in galactic nuclei. We simply may not understand well enough the physical processes of the tidal disruption of stars and the subsequent evolution of the debris.

One of the key questions here is how the stellar debris forms an accretion disk around the black hole and is accreted onto it (Rees 1994). Since the initial orbit of the debris is extremely eccentric, the accretion timescale is longer than the typical interval between two successive tidal disruption events (Gurzadyan & Ozernoy 1980, 1981). But, if the orbit of the debris can be circularized, the accretion timescale can become as short as a few tens of years (Cannizzo et al. 1990). It has been shown that strong relativistic effects make the orbit of the debris stream precess at a large rate around the black hole (on the order of 1 rad per revolution; see, e.g., Rees 1988; Cannizzo et al. 1990; Monaghan & Lee 1994; Kochanek 1994). As a result, the parts of the stream with different orbital periods (we will call them the "outgoing" and "incoming" streams hereafter) may cross each other, and this stream-stream collision may dissipate the orbital energy via a shock, leading to an effective circularization.

So the circularization process through stream-stream collision is a crucial issue in estimating the observational consequences of the tidal disruption of a star. However, the supersonic collision of two gas streams has not been investigated in detail to tell us how the gas flow evolves subsequently and how accretion follows. One can expect that the details of the stream-stream collision and the efficiency of the circularization will depend upon the geometry and flow parameters of the gas streams at the time of the collision. Kochanek (1994) estimated that the widths and heights of the two colliding streams would differ by a factor of 2 or more and that the collision angle between the streams is typically 130°–140°. He suggested that most of the larger stream would freely move away along its original path, because of significantly different cross sections, so that the stream-stream collision should have only small effects on the orbital evolution.

Motivated by this, we have studied the evolution of the

collision of the outgoing and incoming streams and estimated the degree of the conversion of the streams' orbital kinetic energy into other forms of energy. First, we study analytically the collision of two one-dimensional, semi-infinite streams and show how the shock parameters depend on the stream density and velocity. In more realistic situations, the cross sections of the two colliding streams can be very different, and the collision is not necessarily head-on. We have therefore performed three-dimensional numerical simulations of collisions of two supersonic streams with different density ratios, cross-sectional ratios, and collision angles.

In § 2, we present the one-dimensional analytic study. This is followed by the description of the three-dimensional numerical study in § 3. In § 4, we describe the results and implications of the simulations. Conclusions are given in § 5.

2. ONE-DIMENSIONAL PLANE-PARALLEL COLLISION

In this section, we describe the evolution of the collision of two plane-parallel gas streams, for which we can find a simple solution. It tells us some essential features found in the three-dimensional simulations.

Suppose that two one-dimensional, semi-infinite gas streams have densities ρ_1 and ρ_2, pressures p_1 and p_2, and velocities $v_1 > 0$ and $v_2 < 0$ and that they collide at $t = 0$. This is an example of the Riemann problem, where a gas flow containing an arbitrary discontinuity sets into motion. Figure 1 shows the solution of the case where $\rho_1 = 4$, $\rho_2 = 1$, $p_1 = p_2 = 2.4 \times 10^{-6}$, and $v_1 = -v_2 = 0.2$. The adiabatic index is $\gamma = 5/3$. The solution for the postshock regions 3 and 4 can be found from the intersection of the two Hugoniot curves on the so-called (p, v) diagrams for the two shocks (see, e.g., Zeldovich & Raizer 1966). Here the two shocks propagate from both sides of the contact discontinuity. The pressure and velocity are continuous across the contact discontinuity, i.e., $p_3 = p_4$ and $v_3 = v_4 = v_{CD}$, where v_{CD} is the velocity of the contact discontinuity.

Since the shocks are strong [i.e., p_3, $p_4 \gg p_1$, p_2, so $\rho_3/\rho_1 = \rho_4/\rho_2 = (\gamma + 1)/(\gamma - 1)$], we find the following simple relations:

$$p_3 = p_4 = \frac{\gamma + 1}{2} \frac{\rho_1 \rho_2}{(\sqrt{\rho_1} + \sqrt{\rho_2})^2} (v_1 - v_2)^2 , \quad (1)$$

$$v_3 = v_4 = v_{CD} = \frac{\sqrt{\rho_1} v_1 + \sqrt{\rho_2} v_2}{\sqrt{\rho_1} + \sqrt{\rho_2}} , \quad (2)$$

$$u_1 = -\frac{\gamma + 1}{2} \frac{\sqrt{\rho_2}}{\sqrt{\rho_1} + \sqrt{\rho_2}} (v_1 - v_2) , \quad (3)$$

$$u_2 = \frac{\gamma + 1}{2} \frac{\sqrt{\rho_1}}{\sqrt{\rho_1} + \sqrt{\rho_2}} (v_1 - v_2) . \quad (4)$$

Here u_1 and u_2 are the shock velocities relative to the upstream flows in regions 1 and 2 (see Fig. 1), respectively. The ratio of the shock velocities is $|u_1/u_2| = \rho_2/\rho_1$, so the ram pressures of the two shocks are same ($\rho_1 u_1^2 = \rho_2 u_2^2$).

One can define the *thermal energy conversion flux*, F_{th}, as the postshock thermal energy generated by the shock per unit area per unit time, according to

$$F_{th} = \frac{p_3}{\gamma - 1} (w_2 - w_1) . \quad (5)$$

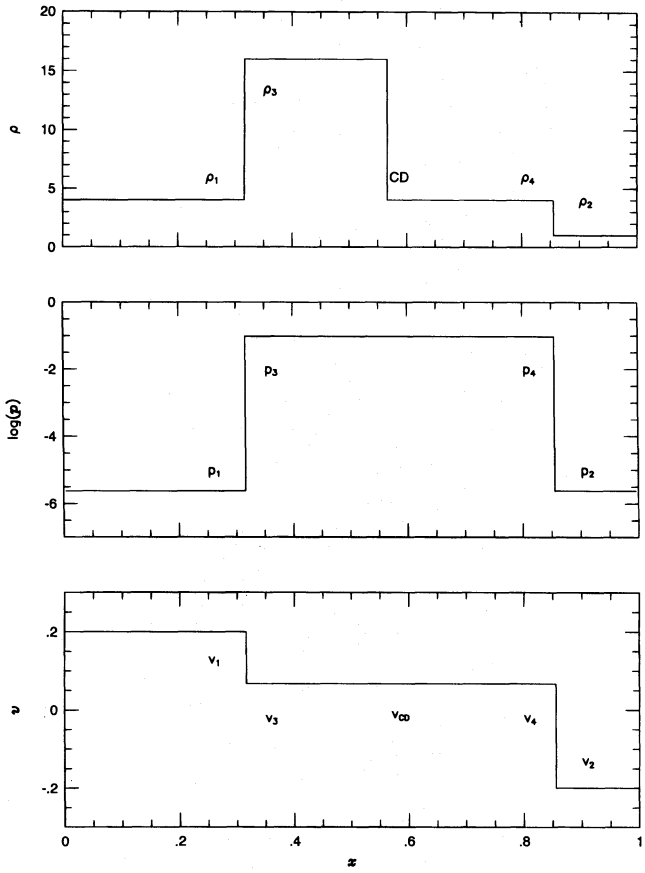

FIG. 1.—Flow structure after the collision of one-dimensional plane-parallel gas streams. The flow parameters ρ_1, p_1, v_1 and ρ_2, p_2, v_2 represent the initial conditions to the left and right of the discontinuity, respectively. Two shocks propagate away from the discontinuity.

Here $w_1 = u_1 + v_1$ and $w_2 = u_2 + v_2$ are the shock velocities in the frame in which the initial flows are defined. In the strong-shock limit,

$$F_{th} = \frac{\gamma + 1}{4} \frac{\rho_1 \rho_2}{(\sqrt{\rho_1} + \sqrt{\rho_2})^2} (v_1 - v_2)^3 . \quad (6)$$

Then the *conversion ratio*, R, can be defined as the ratio of the thermal energy conversion flux to the influx of the kinetic energy; that is,

$$R = \frac{F_{th}}{(1/2)\rho_1 v_1^3 + (1/2)\rho_2 v_2^3} . \quad (7)$$

The probable configuration for the collisions of the debris streams mentioned in § 1 is the one with $\chi = \rho_1/\rho_2 \gtrsim 1$ and $v_2 \sim -v_1$. In this case, $|u_1/u_2| = \sqrt{\chi}$. Then the postshock pressure is given by

$$p_3 = \frac{\gamma + 1}{2} \rho_2 (v_1 - v_2)^2 \frac{\chi}{(\sqrt{\chi} + 1)^2} \quad (8)$$

if the shocks are strong. The term $\chi/(\sqrt{\chi} + 1)^2$ varies from $\frac{1}{4}$ to 1 for $\chi \geq 1$. Thus the postshock pressure is determined mostly by the relative velocity of the gas streams and the density of the lower density stream, but it is almost independent of the density of the higher density stream. Since $F_{th} \propto p_3(v_1 - v_2)$, the thermal energy conversion flux is also determined by the density of the lower density stream. The con-

TABLE 1

MODEL PARAMETERS

Model	θ	ρ_1/ρ_2	r_1/r_2
A18	18°	1	7/7
A26	26	1	7/7
A36	36	1	7/7
A45	45	1	7/7
A52	52	1	7/7
A63	63	1	7/7
A71	71	1	7/7
A90	90	1	7/7
A126	126	1	7/7
A143	143	1	7/7
A180	180	1	7/7
B143a	143	4	5/10
B143b	143	9	3/9
B143c	143	16	3/12
B180	180	16	3/12

version rate R decreases with increasing χ, so the energy conversion is less efficient if the density contrast is large. In the limit of high χ ($\chi \rightarrow \infty$), the collision of two streams reduces effectively to a problem in which a solid body is moving into a low-density stream. Then only one *bow* shock propagates into the low-density medium, and the postshock pressure is the ram pressure on the solid body. The contact surface moves with the velocity of the solid body.

Another extreme case is the one in which the colliding gas streams are identical ($\chi = 1$) and have opposite velocities, $v_2 = -v_1$. Then the postshock regions have $p_3 = p_4 = 4\rho_1 v_1^2/3$ and $v_3 = v_4 = 0$, and the shock speeds relative to the upstream flows are $u_1 = -u_2 = -4v_1/3$. The thermal energy conversion flux is $F_{\rm th} = 4\rho_1 v_1^3/3$, and the conversion ratio is $R = 4/3$, which is the largest value attained. The reason R is greater than 1 can be understood as follows: All the kinetic energy of the gas that passes through the shock is converted into thermal energy since the postshock gas is at rest in the lab frame. But the shocks move outward from the contact point, so $R = |u_1/v_1|$, which is 4/3 for $\gamma = 5/3$.

3. THREE-DIMENSIONAL HYDRODYNAMIC SIMULATIONS

We are interested in the situation in which the gas streams move into an extremely low-density and low-pressure medium with a supersonic speed. For numerical simulations, however, we have adopted flow parameters that can be handled comfortably with our code. In the collisions of two identical streams, we have set $\rho = 1$, $p = 2.4 \times 10^{-6}$, and $v = 0.2$ for the streams, so the Mach number is $v/c_s = 100$. Since the colliding gas is cold, collisions with a higher Mach number would represent a more realistic situation. It is expected that the streams of stellar debris may have cross sections inversely proportional to the density, i.e., $\sigma\rho$ = constant, while they have similar orbital speeds (Kochanek 1994; Monaghan & Lee 1994). Thus, in the collisions of two different streams, we vary the density and the cross section according to $\sigma\rho$ = constant. We use $\rho_2 = 1$ for the low-density stream, and the density contrast is $\chi = \rho_1/\rho_2 = \sigma_2/\sigma_1 = 4$, 9, or 16. The speed and pressure are the same, that is, $v_1 = v_2 = 0.2$ and $p_1 = p_2 = 2.4 \times 10^{-6}$. For the density contrasts considered here ($\chi =$ 4–16), we expect that the results would be somewhere between those of identical streams ($\chi = 1$) and those for a high density contrast ($\chi \rightarrow \infty$).

The density and pressure of the ambient medium are set to $\rho_b = 10^{-3}\rho_1$ and $p_b = 10^{-3}p_1$. Since the pressure of the stream is higher than that of the ambient medium, a shock propagates into the ambient medium and a rarefaction wave propagates into the stream. But the shock is weak, with Mach number $u_{\rm ps}/c_b = 1.8$, where c_b is the sound speed of the ambient medium. If the ambient medium is a vacuum, the shock has a maximum speed $u_{\rm ps} = 2c_b/(\gamma - 1)$. However, the maximum shock speed is still much smaller than the stream speed, so the shock propagating from the stream boundary is not dynamically important at all.

For the boundary condition on the streams, we have used the inflow condition that the flow variables of the streams entering the computational domain are continuous across the boundary (i.e., no gradient). This inflow condition can be handled exactly only when the inflow angle relative to the boundary is given by $\tan\theta_{\rm in} = n_1/n_2$, where n_1 and n_2 are integers from 0 to ∞. Hence in our simulations we consider only collisions with collision angles given by $\tan\frac{1}{2}\theta = \frac{1}{3}, \frac{1}{2}, 1, 2, 3$, and ∞. The most likely collision angle between the outgoing and incoming gas streams expected around a black hole is greater than 90°—more restrictively, between 130° and 140°, as mentioned in § 1. So we pay special attention to the cases $\theta = 143°$ and $\theta = 180°$.

We divide the simulations into two groups. Group A is for the simulations with two *identical* streams colliding with different collision angles. So model "A36," for example, is for the collision of two identical streams with the collision angle 36°. Group B is for the simulations with two *different* streams colliding at either 143° or 180°. The stream parameters, such as the ratios of the densities and radii of the cross-sectional areas of the two streams, are listed in Table 1.

The simulations were performed with a three-dimensional hydrodynamics code based on the total variation diminishing (TVD) scheme (Harten 1983; Ryu et al. 1993). This is an explicit, second-order, Eulerian finite-differencing scheme. In the simulations with the TVD code, shocks spread over two to three cells. In our simulations, the computational box is a unit cube, typically with 128^3 cells. Since the fast stream has a speed of 0.2, it can cross the box in $t = 5$. The streams have been set to collide at $t = 0$, and the temporal integration has been calculated up to $t = 2.0$. A typical run takes $\lesssim$1000 CPU seconds on a Cray C90.

4. RESULTS AND IMPLICATIONS

4.1. *Morphology*

Let us start with an overview of the morphological shape in the stream-stream collisions. To see some of the key features described in the following, refer to Figures 2–5. Figure 2 shows the pressure contour maps of a slice cut through the middle plane of the colliding streams for four models in group A (A18, A36, A90, and A180). Figure 3 shows the pressure contour maps for models with $\theta = 143°$ (i.e., A143, B143a, b, c). The density contour maps for the same models as shown in Figure 3 are plotted in Figure 4. Figure 5 shows the velocity maps for models A143, B143c, A180, and B180. Morphologically, the most noticeable feature is the oblique shocks formed around the contact surface. They can be identified by strong gradients in the pressure contour maps.

For a collision of two identical streams, one can define a symmetry plane that contains the initial contact surface. The angle between the oblique shocks and the symmetry

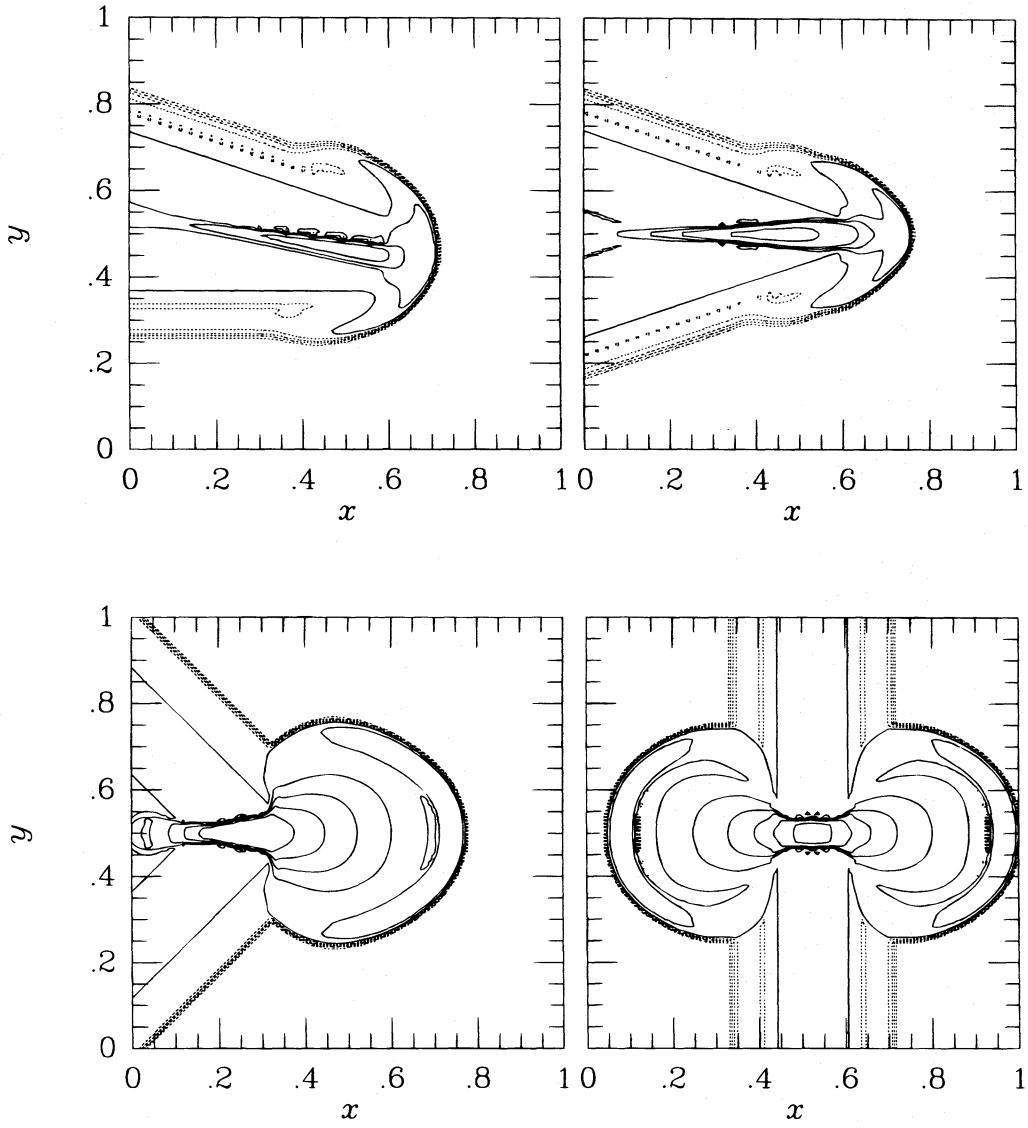

FIG. 2.—Pressure contour maps of a horizontal cut in models A18 (*top left*), A36 (*top right*), A90 (*bottom left*), and A180 (*bottom right*)

plane depends on the flow parameters and the collision angle. This angle is zero for the collision angle $\theta = 180°$ and increases up to a maximum angle of $\sim 11°$ as θ decreases to 90°. Then it decreases as the collision angle further decreases below 90°. Once the angle between the oblique shocks and the symmetry plane is known, the shock jump condition can be found by applying the usual Hugoniot-Rankine relations. As the collision angle increases, the velocity component perpendicular to the symmetry plane increases, so the postshock gas pressure behind the oblique shock increases.

The collision of two identical streams at collision angle $\theta = 180°$ (model A180) is most closely comparable to the one-dimensional collisions considered in § 3. In the one-dimensional collisions, the shocks propagate back to the upstream flows, and the shock speed relative to the upstream flows is $4v_{st}/3$. But in the three-dimensional collisions, the shock speed is $\sim v_{st}$ since the shocks stand off near the symmetry plane instead of penetrating into the upstream flows. This is because the high pressure behind the shocks pushes the shocked gas into the low-pressure ambient medium in the direction perpendicular to the stream flows. The shocked gas is first accumulated into a dense region between the shocks and then accelerated into the ambient medium. This expanding hot gas drives another shock into the ambient medium. This secondary shock is identified by strong pressure gradients in the background medium. The speed of this shock is similar to the stream speed itself since the postshock pressure is similar to the ram pressure of the streams. The high-pressure shocked region is roughly divided into a small volume of the densest gas surrounded by main shocks and a large volume of diffuse, expanding flow encompassed by the secondary shock.

In the cases with collision angle greater than 90° but less than 180° (e.g., A143), a forward shock and a reverse shock propagate into the two directions in the ambient medium. The forward shock moves faster than the reverse shock because of the positive bulk motion of the streams along the symmetry plane. The three-dimensional shape of the expanding high-pressure region is then a torus that encompasses the contact surface, but the cross section of the torus is not symmetric. When the collision angle is smaller than 90° (see Fig. 2), the reverse shock is absent.

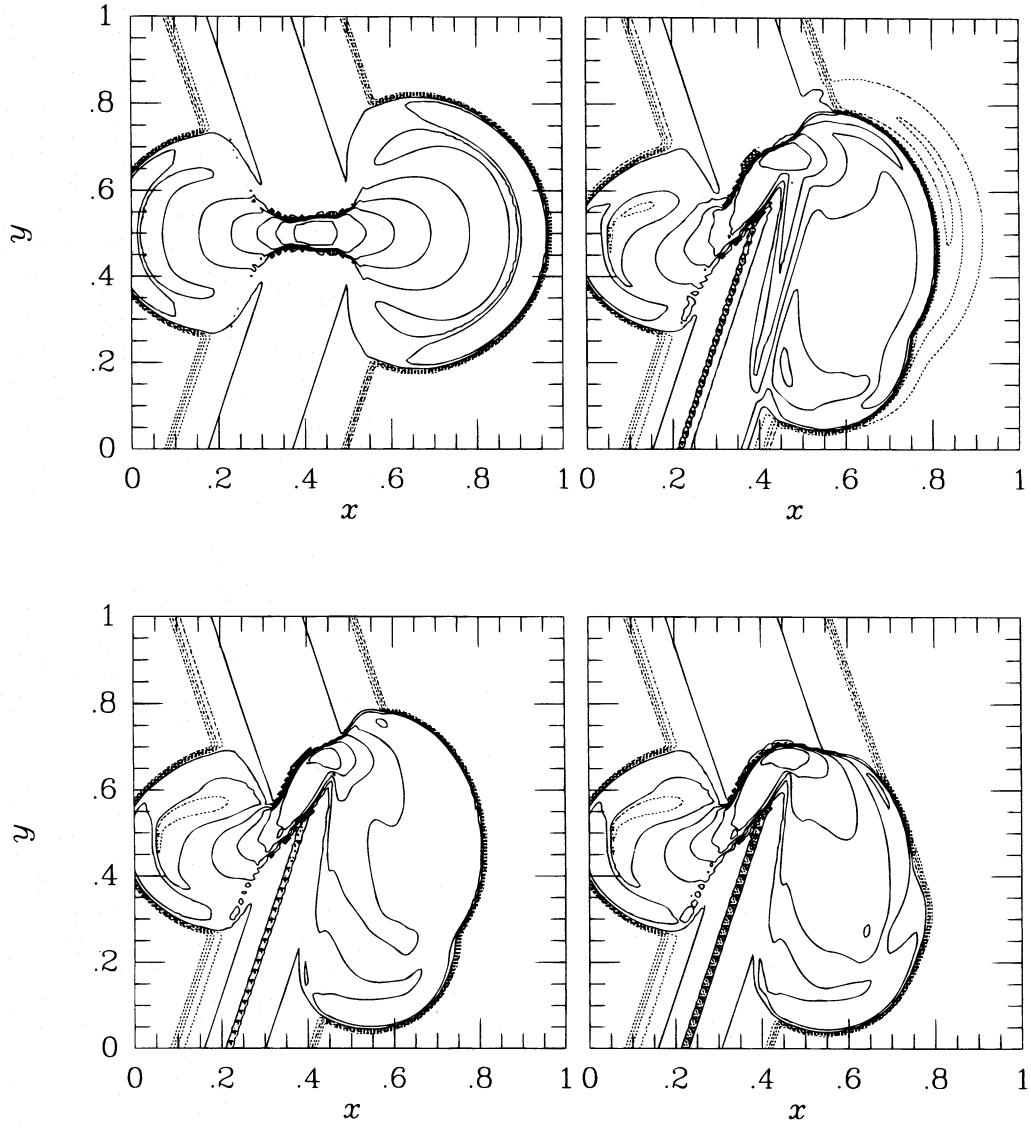

FIG. 3.—Pressure contour maps of a horizontal cut in models A143 (*top left*), B143a (*top right*), B143b (*bottom left*), and B143c (*bottom right*)

In the collisions of two different streams (B143a, b, c, and B180), the high-density stream penetrates somewhat into the low-density stream since the high-density stream has a smaller cross section. However, the oblique shocks extend beyond the overlapping contact surface, which is determined by the cross section of the high-density stream. The flow outside the overlapping contact surface is prevented from streaming freely by the extended, oblique shocks and the torus of the high-pressure gas. Hence, contrary to a naive expectation, the geometric cross section of interacting streams seems to have a rather weak influence on the dynamics of stream-stream collisions.

4.2. *Energy Conversion*

The component of the orbital kinetic energy of the streams due to the motion perpendicular to the oblique shocks is converted to thermal energy by heating the shocked gas. But the heated gas expands into the ambient medium and cools adiabatically. Through this adiabatic expansion, the thermal energy is converted back to the kinetic energy of the expanding gas encompassed by the secondary shocks, as described in § 4.1. In order to quantify the efficiency of the conversion of the stream's orbital kinetic energy into thermal energy, we define the energy conversion rate, R, as the ratio of the increase in the total thermal energy in the computational box to the kinetic energy added to the box through the boundary, i.e.,

$$R = \frac{U_{\rm tot}(t) - U_{\rm tot}(0)}{(1/2)\rho_1 v_1^2(\sigma_1 v_1 t) + (1/2)\rho_2 v_2^2(\sigma_2 v_2 t)}, \qquad (9)$$

where $U_{\rm tot}(t)$ is the total thermal energy at t. This ratio has a meaning similar to the conversion rate defined in equation (7). Values of R for various models are plotted against t in Figure 6. The slow increase in R during the early phase for $\theta < 180°$ is due to the fact that the area of the contact surface increases with time. The subsequent decrease is due to the following reason: The total thermal energy $U_{\rm tot}(t)$ increases initially with t, but then stays more or less constant after the contact surface is fully developed. But the kinetic energy in the denominator of equation (9) continues to increase with time, so the ratio R decreases at late epochs. At the end of our simulations ($t = 2$), only a small fraction

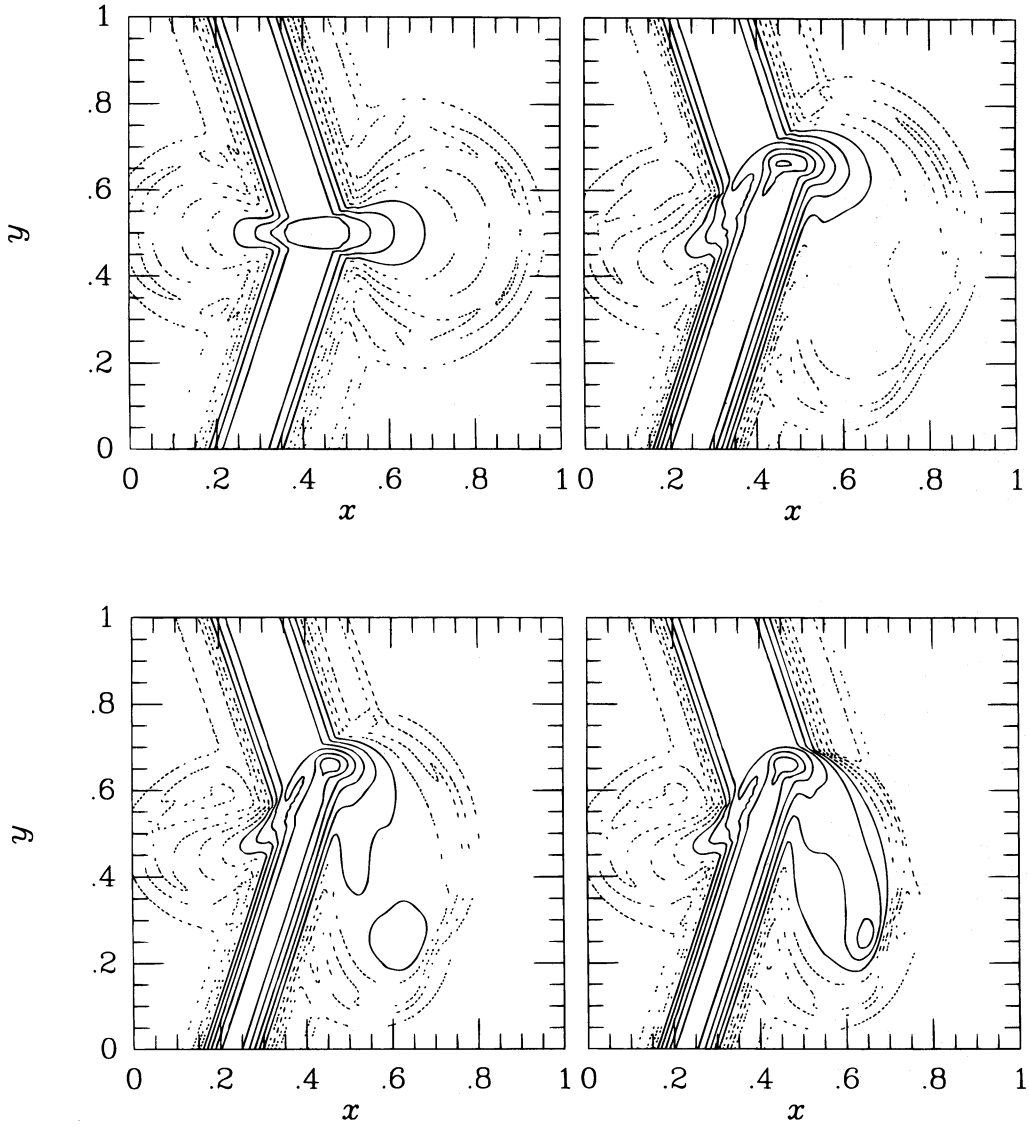

FIG. 4.—Density contour maps of a horizontal cut in models A143 (*top left*), B143a (*top right*), B143b (*bottom left*), and B143c (*bottom right*)

of the stream's orbital kinetic energy ($\lesssim$30%) was converted to thermal energy, and most of it went to the kinetic energy associated with expansion of the hot torus gas.

Since the initial orbital energy of the streams is converted eventually to the expansion energy of the shocked gas, the nature of the debris' orbit would change drastically after the stream crossing. The amount of energy transferred to the expanding motion can be estimated from the maximum value of the energy conversion rate. If the maximum R is close to 1, almost all the stream's orbital energy will eventually be converted into the expansion energy. In the cases of the collision of two identical streams, the maximum R is generally close to 1. The maximum R becomes smaller as the cross-sectional area (and thus density) contrast grows, but the dependence is rather weak. For example, the maximum R of the different-stream cases (for $\chi = 4$–16) are $\sim$30%–35% of that of the identical-stream case (see Fig. 6). Thus the conversion of the orbital energy to the expansion energy is still significant unless the density contrast is very large (i.e., $\chi \gg 10$). This is mainly due to the fact that the oblique shocks affect the area beyond the overlapping contact surface, as discussed in § 4.1. A similar level of decrease in the energy conversion with density contrast can be seen in the bottom right panel of Figure 6 ($\theta = 180°$), where head-on collision cases are shown.

4.3. *Implications on the Long-Term Evolution of Stellar Debris*

The simulations of two-stream collisions comprise only a small part of the evolution of stellar debris around a black hole, but we may still extract some important physics. In this subsection, we attempt to predict how the collision of debris streams affects their evolution, and how the circularization of the debris' orbit proceeds, by relating the results of the present simulations to those of the stellar disruption simulations described in Monaghan & Lee (1994).

In Figure 7, we show a typical geometry of gas streams resulting from an SPH simulation for the disruption of a star near a black hole (Monaghan & Lee 1994). The arrows indicate the direction and size of the SPH particles' velocity. The magnitude of the velocity of the streams is close to the escape velocity, because the eccentricity is almost 1. Therefore, at a distance r from the black hole, it can be approximated as

$$v \approx \sqrt{2GM/r}\,, \tag{10}$$

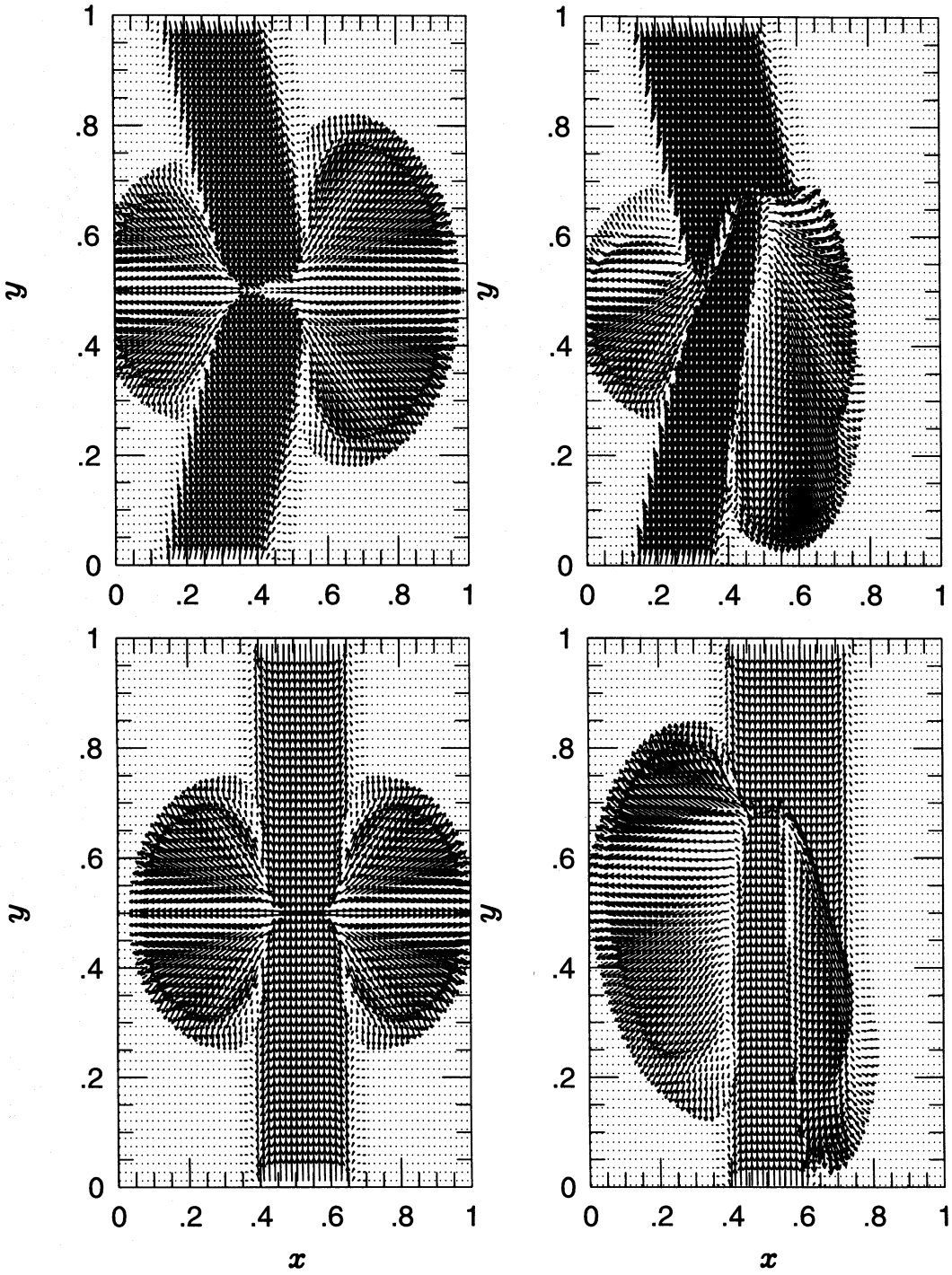

FIG. 5.—Velocity field maps of a horizontal cut in models A143 (*top left*), B143c (*top right*), A180 (*bottom left*), and B180 (*bottom right*)

where M is the mass of the black hole. The angle of the stream crossing is approximately given as

$$\theta \approx \pi(1 - 1.5R_S/r_p)\,, \tag{11}$$

where r_p is the pericentric distance of the orbit of the disrupted star and R_S is the Schwarzschild radius of the black hole. Here we have assumed that the velocity vector at the crossing is nearly *radial*. The relation given by equation (10) can be confirmed from Figure 8, where we have shown the velocity of SPH particles as a function of distance from the black hole. (Note that the length unit shown in Figs. 7 and 8 is $\frac{1}{2}R_S$.) In Figure 8, the circles denote the outgoing particles while the crosses represent the incoming particles. There is no distinction in orbital velocities for the incoming and outgoing particles. Since the location of the stream crossing is about $r_{cr} = 50R_S$ (or 100 in the present length unit) from the black hole, it can be seen that the velocities are closely approximated by equation (10). With a typical value of $r_p \approx r_{tid} \approx 5R_S$, we obtain $\theta \approx 130°$, where r_{tid} is the tidal disruption distance.

We can estimate the average velocity of the shocked streams along the tangential direction as $v_{tan} \sim v_{st}(2 \cos$

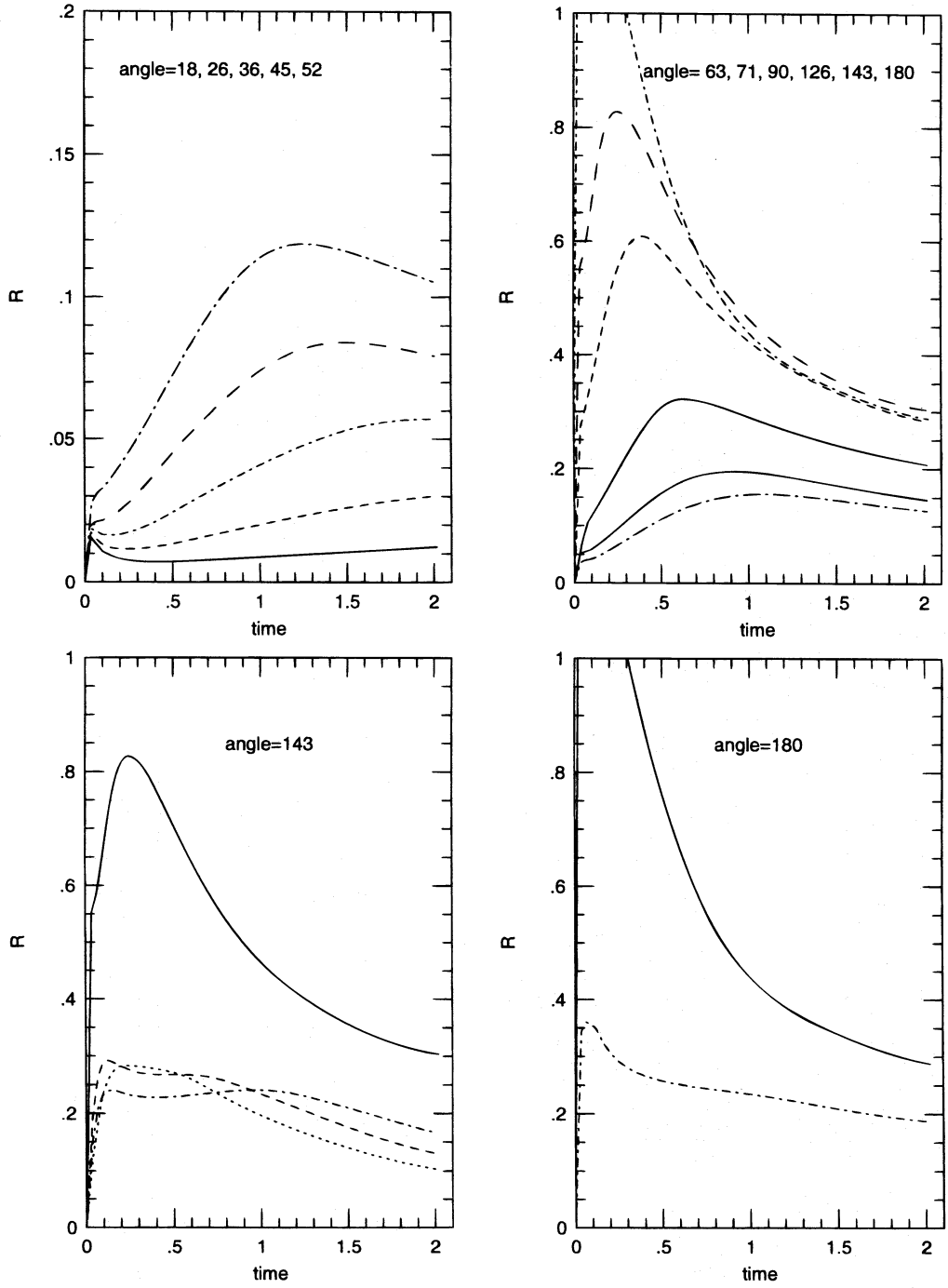

FIG. 6.—Energy conversion rate R. The top two panels are for the models with two identical streams. R increases with the collision angle. The bottom left panel is for the models with the collision angle 143°; the solid line is for model A143 (i.e., identical streams), the dotted line for B143a ($\chi = 4$), the dashed line for B143b ($\chi = 9$), and the dot-dashed line for B143c ($\chi = 16$). The bottom right panel is for the models with the collision angle 180°; the solid line is for A180 (i.e., identical streams), the dot-dashed line for B180 ($\chi = 16$).

$\frac{1}{2}\theta)^{1/2}$ for the collision of two identical streams if we assume that the collision is *sticky* (i.e., inelastic) and that the gas is incompressible. It is equal to the circular velocity $v_{\rm cir} = (GM/r)^{1/2}$ for $\theta \approx 151°$. Thus for the typical angle of $\theta \approx 130°$, the tangential velocity of the sticky, incompressible fluid will be close to the value for a circular orbit. In such case the orbital energy would be removed effectively, and the shocked gas would move in a nearly circular orbit at the orbital radius $r_{\rm cr}$. In reality, however, the gas is neither sticky nor incompressible, so the shocked gas goes through an adiabatic expansion.

The geometry of the crossing debris streams would resemble that somewhere between A143 and B143c (see Figs. 3, 4). In Figure 9 we show the accumulated frequency distribution of the kinetic energy per unit mass (E_k) for all the gas within our simulation box at the end of our runs of models A143a and B143c. The kinetic energy of the initial streams ($E_{k,s}$) is indicated as a vertical line at $E_k/E_{k,s} = 1$. The presence of gas at both lower and higher sides of the initial E_k is due to the shock. The bulk of the shocked gas has energy smaller than the initial stream's kinetic energy. Thus the stream crossing will make the shocked gas more

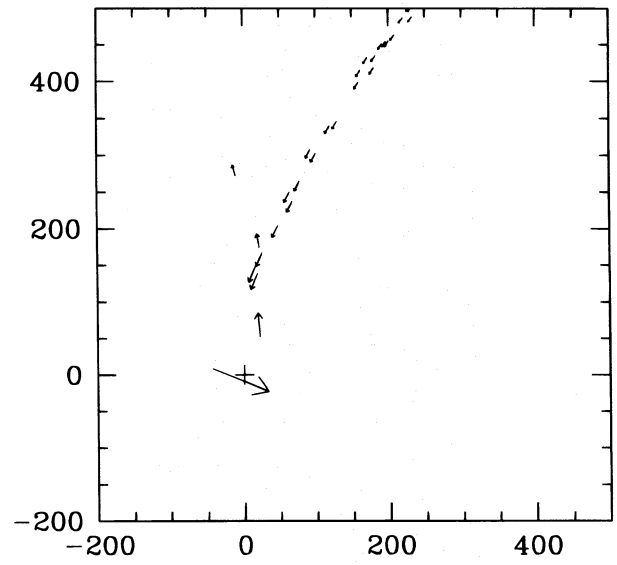

FIG. 7.—Typical geometry of stream crossing resulting from an SPH simulation. The arrows indicate the locations and velocities of SPH particles. The length unit in this figure is $\frac{1}{2}R_S$.

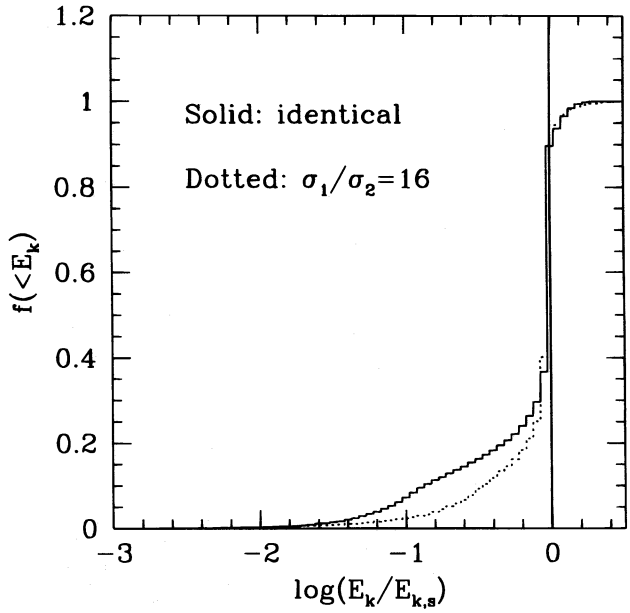

FIG. 9.—Accumulated frequency distribution of kinetic energy per unit mass (E_k) for all the gas in our simulation box at the end of simulations for models A143 and B143c. The kinetic energy of the incoming stream is indicated as a vertical line at $E_k/E_{k,s} = 1$. The majority of the shocked gas has lost its kinetic energy while a small fraction has gained it.

tightly bound to the black hole. A small fraction of the shocked gas has kinetic energy greater than that of the initial streams, as evident from the high-velocity tail in Figure 9. The amount of gas having $E_k > E_{k,s}$ is $\sim\frac{1}{4}$ of that with $E_k < E_{k,s}$. However, the majority of the high-velocity gas still lies very close to $E_{k,s}$, so the fraction of gas that will be unbound from the black hole is likely to be very small (<10%).

The difference in circularization efficiency between the identical- and different-stream collisions can also be noted from Figure 9. About half the gas with $E_k < E_{k,s}$ has $E_k < 0.5E_{k,s}$ for model A143a, while the fraction becomes less than $\frac{1}{3}$ for model B143b. $E_k = 0.5E_{k,s}$ represents approximately the energy of the gas that has a circular orbit after the shock. Thus the particles with $E_k < 0.5E_{k,s}$ have an apocenter smaller than r_{cr} while those with $E > 0.5E_{k,s}$ have an apocenter greater than r_{cr}.

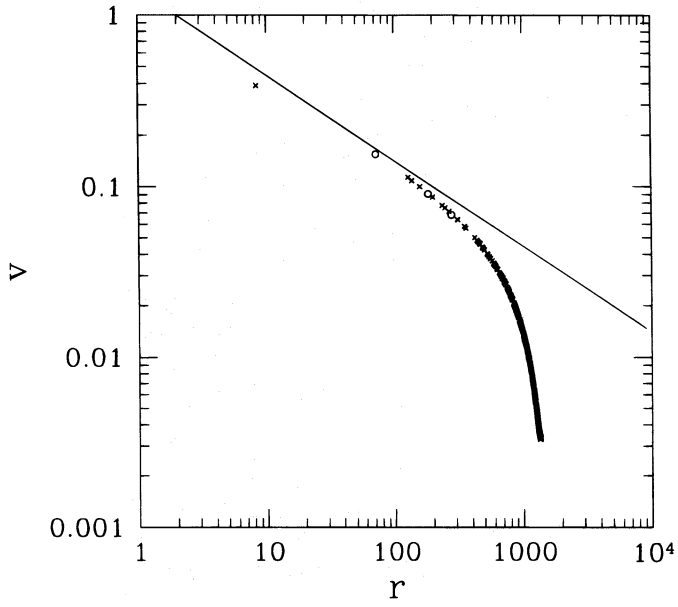

FIG. 8.—Velocity of SPH particles as a function of distance from the black hole for the case shown in Fig. 7. The straight line indicates the v-r relationship for a parabolic orbit.

Once the stream crossing begins, the incoming stream no longer exists beyond the crossing point. The tail of the incoming stream moves around the black hole and becomes the endpoint of the outgoing stream. After the tail of the outgoing stream is destroyed by the collisions, the incoming stream will flow freely again. Thus the duration of a stream-stream collision until the exhaustion of one segment of the outgoing stream is about the time required for a particle to have a round trip from the location of the stream crossing through the apocenter from the black hole. For a particle with a nearly parabolic orbit, the duration is twice the free-fall time. Thus the collision timescale would be $t_{col} \approx 2[3\pi^2 r^3/(8GM)]^{1/2} \sim 50$ hr for our choice of typical parameters (i.e., $M = 10^7\ M_\odot$, $r_{cr} \approx 50R_S$, and $r_p \approx r_{tid} \approx$ 1 AU). The quiescent phase would have a similar duration. Therefore, the stream collision could be a periodic phenomenon with period $\sim$100 hr. A tidal disruption with smaller r_p would produce a shorter period, because r_{cr} is smaller. Obviously, such a periodicity is less pronounced if the contrast in cross-sectional areas becomes larger.

5. CONCLUSION

We have investigated supersonic collisions between two gas streams with various configurations and collision geometries. In the collisions of one-dimensional plane-parallel streams, the kinetic energy is converted effectively into thermal energy via the shocks that propagate into the streams. The conversion is most effective for the collision of two identical streams. It becomes least effective if the two streams have an infinite density contrast. For the intermediate density contrast, the thermal energy conversion is proportional to the ram pressure of the low-density stream but nearly independent of that of the high-density stream. If the shocked gas can cool radiatively on a timescale shorter than

the dynamical time, the kinetic energy of the streams would be dissipated more effectively.

The collisions of three-dimensional streams are much more complicated. We have more degrees of freedom in setting flow parameters, such as the ratio of cross sections and collision angle. The key features of the three-dimensional simulations that contrast with the one-dimensional collisions include: (1) The shocks generated by the collisions remain near the standoff point instead of penetrating into the colliding streams. (2) Most of the bulk kinetic energy of the streams turns into the kinetic energy of the expanding hot gas instead of thermal energy. (3) The hot gas behind the shock expands uniformly in the directions perpendicular to the colliding streams.

In the collision of two identical streams, the fraction of orbital kinetic energy converted into the kinetic energy of expansion is high, so the circularization is effective. But realistic streams at the crossing point are likely to have a density contrast as large as ~ 4–10, and the ratio of cross sections is expected to vary as the reciprocal of the density contrast. In such cases, the conversion of the orbital kinetic energy should be somewhat smaller. If we quantify the circularization efficiency by the fraction of the orbital kinetic energy transferred to the kinetic energy of expansion, the efficiency would be nearly 50% for B143a ($\chi = 4$) and B143b ($\chi = 9$) and 30% for B143c ($\chi = 16$), while nearly 100% for A143 ($\chi = 1$). The reason that the circularization efficiency depends only weakly on the ratio of cross sections is that the shock-heated gas forms a *thick torus* of high-pressure gas, which keeps the stream of larger cross section from streaming freely. Thus stream-stream collision could still be an effective circularization mechanism, even if the ratios of densities and cross sections of two streams are significant ($\chi \lesssim 10$).

The detailed evolution of the expanding gas under the gravity of the black hole is still complicated. Some would escape from the black hole's gravity, taking energy away with it and leaving the debris more tightly bound to the black hole. Therefore, the collision could be considered as an effective way to dissipate the orbital kinetic energy of the streams, even in the absence of the radiative cooling of the shocked gas.

The stream crossing would last for a while (~ 50 hr for typical parameters, i.e., $M = 10^7\ M_\odot$, $r_{\rm cr} \approx 50 R_{\rm S}$, and $r_p \approx r_{\rm tid} \approx 1$ AU), with a similar period of quiescence following. Such a pattern is likely to repeat until the majority of stellar debris returns to the apocenter. Thus a periodic occurrence of *flare* could be observed if the stream crossing can produce any observable phenomena.

So far, we have considered an adiabatic gas with adiabatic index $\gamma = 5/3$ and ignored any radiative processes. In the collision of two gas streams, however, their kinetic energy could go mostly into radiation pressure rather than gas pressure, depending on the parameters. In such cases, $\gamma = 4/3$ would be more appropriate than $\gamma = 5/3$. But we believe that this is unlikely to make much of a difference to the overall outcomes of our calculations. Also, it is possible that radiative processes might be important. For instance, if the torus of the shocked gas is optically thin, radiative losses could efficiently take away internal energy almost instantaneously as it is created in the shocks. There, isothermality might be a better approximation. If it is optically thick, on the other hand, the radiative viscosity might play an important role. Since we have limited ourselves to the dynamics of an adiabatic gas in the present paper, we leave these to future works.

We thank T. W. Jones and J. Goodman for comments on the manuscript. The work by H. M. L. was supported in part by KOSEF grant 941-0200-001-2 and in part by the Cray Research and Development Grant in 1994. The work by H. K. was supported in part by the Korea Research Foundation through the Brain Pool Program. The work by D. R. was supported in part by the Basic Science Research Institute Program, Korean Ministry of Education 1995, project BSRI-95-5408.

REFERENCES

Cannizzo, J., Lee, H. M., & Goodman, J. 1990, ApJ, 351, 38
Goodman, J., & Lee, H. M. 1989, ApJ, 337, 84
Gurzadyan, V. G., & Ozernoy, L. M. 1980, A&A, 86, 315
———. 1981, A&A, 95, 39
Harten, A. 1983, J. Comput. Phys., 49, 357
Kochanek, C. S. 1994, ApJ, 422, 508
Monaghan, J. J., & Lee, H. M. 1994, in The Nuclei of Normal Galaxies, ed. R. Genzel & A. I. Harris (NATO ASI Ser. C, 445) (Dordrecht: Kluwer), 449
Rees, M. J. 1988, Nature, 333, 523
———. 1994, in The Nuclei of Normal Galaxies, ed. R. Genzel & A. I. Harris (NATO ASI Ser. C, 445) (Dordrecht: Kluwer), 453
Ryu, D., Ostriker, J. P., Kang, H., & Cen, R. 1993, ApJ, 414, 1
Zeldovich, Ya. B., & Raizer, Yu. P. 1966, Physics of Shock Waves and High-Temperature Hydrodynamic Phenomena (New York: Academic)